Contents of this file

1. Section S1: Introduction
2. Figures S1-S8
3. Tables S1-S3

S1 Introduction

This supporting information contains eight figures and three tables. Figures S1–S4 present histograms based on the posterior distributions of the calibrated parameters estimated in the Markov chain Monte Carlo simulation with MyLake C using each gas exchange model and their respective prior probability distributions. Figure S5 shows the simulated gas transfer velocities and air-water CO_2 fluxes with each version of the MyLake C application. Figure S6 displays the simulated and measured water column temperatures at the calibration depths. Figure S7 presents the simulated and measured components of the effective surface heat flux. Figure S8 shows the simulated and measured atmospheric friction velocities over the lake. Table S1 presents the results of the performance assessment of the CO_2 simulations with each version of the model application during model calibration and validation. Table S2 presents the results of the performance assessment of the simulation of the components of effective surface heat flux. Table S3 presents the performance assessment results for near-surface CO_2 concentration, gas transfer velocity for CO_2, and air-water CO_2 flux obtained with each version of the model application.

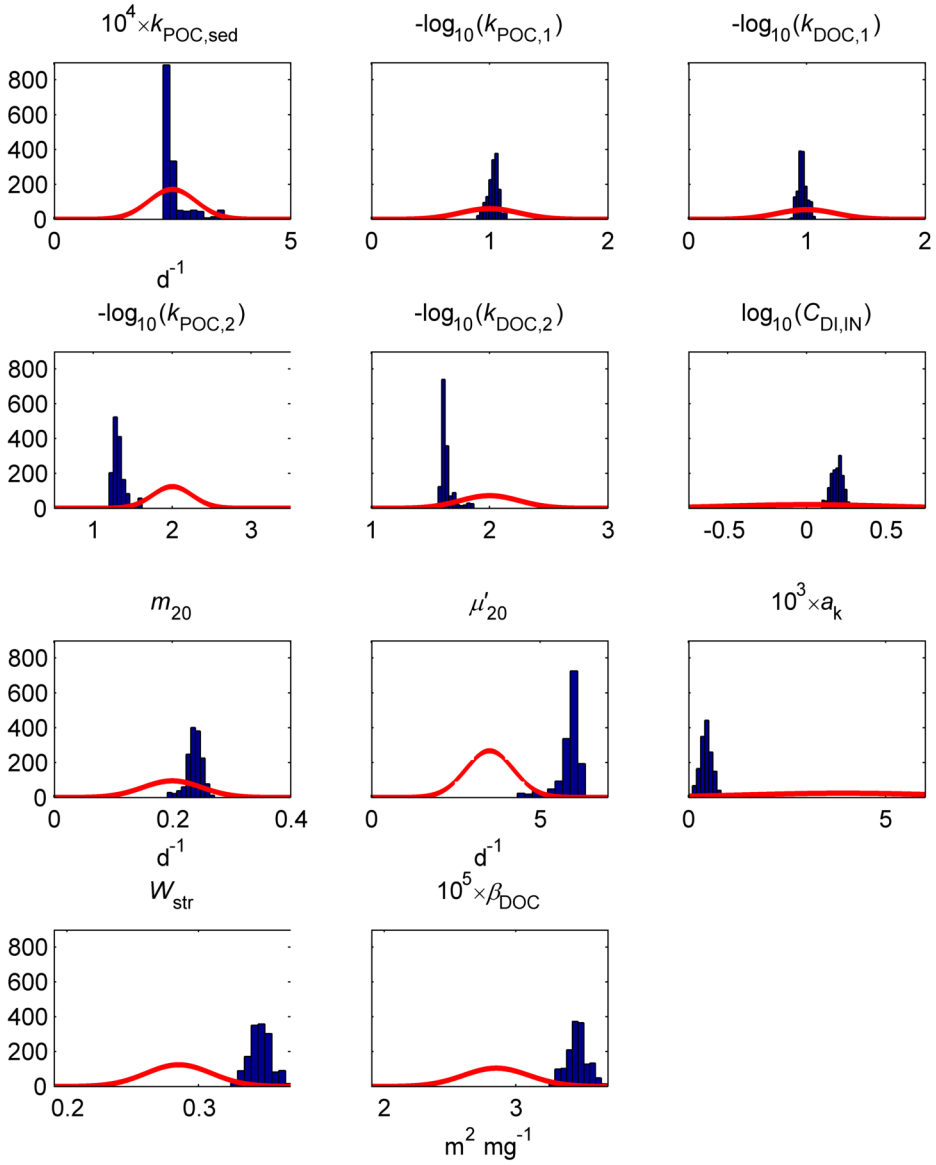

Figure S1. Histograms based on the posterior distributions of the 11 calibrated parameters (blue bars) estimated in the Markov chain Monte Carlo simulation with MyLake C using the gas exchange model by Cole and Caraco (1998) and their prior probability distributions (red lines). The histograms were calculated using the latter half of the parameter chain with a length of 3000 iterations.

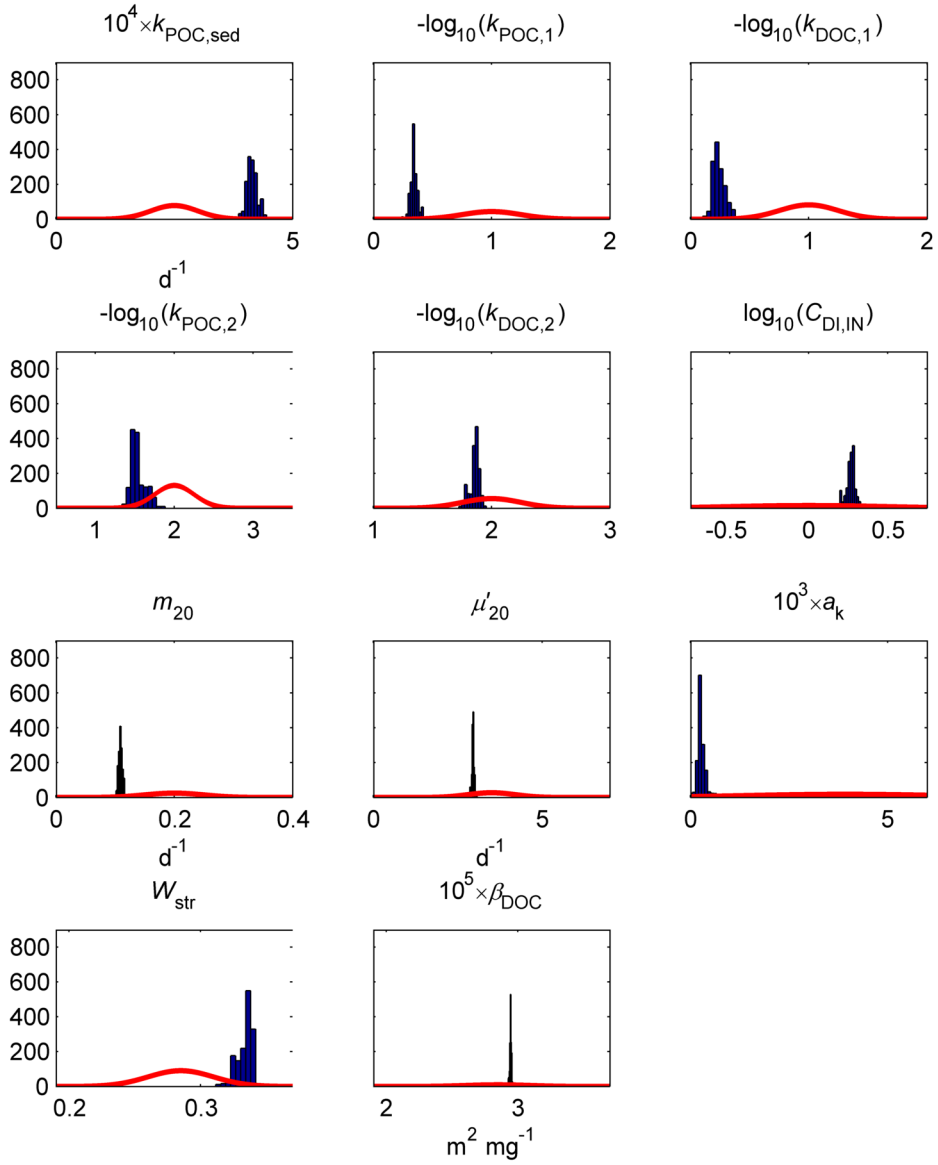

Figure S2. Histograms based on the posterior distributions of the 11 calibrated parameters (blue bars) estimated in the Markov chain Monte Carlo simulation with MyLake C using the gas exchange model by Heiskanen et al. (2014) and their prior probability distributions (red lines). The histograms were calculated using the latter half of the parameter chain with a length of 3000 iterations.

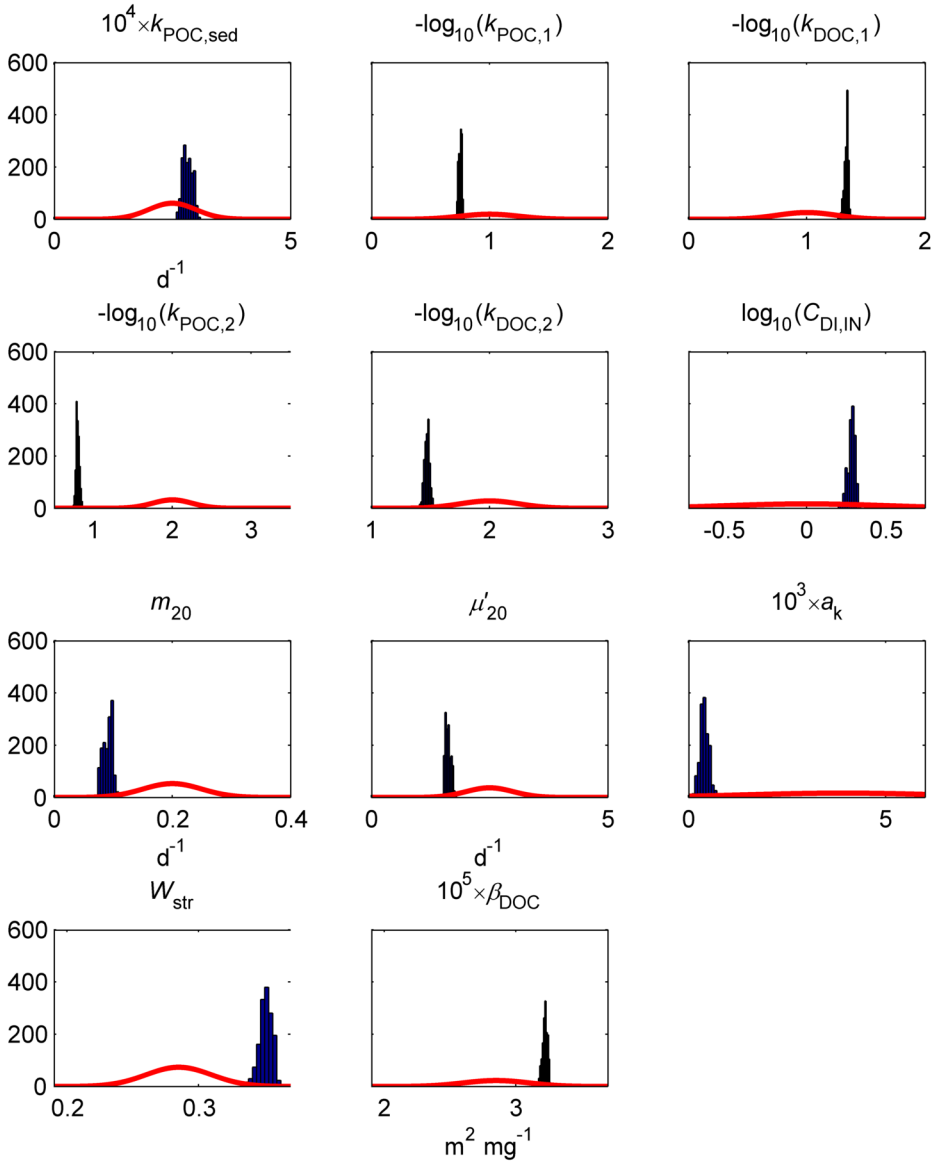

Figure S3. Histograms based on the posterior distributions of the 11 calibrated parameters (blue bars) estimated in the Markov chain Monte Carlo simulation with MyLake C using the gas exchange model by MacIntyre et al. (2010) and their prior probability distributions (red lines). The histograms were calculated using the latter half of the parameter chain with a length of 3000 iterations.

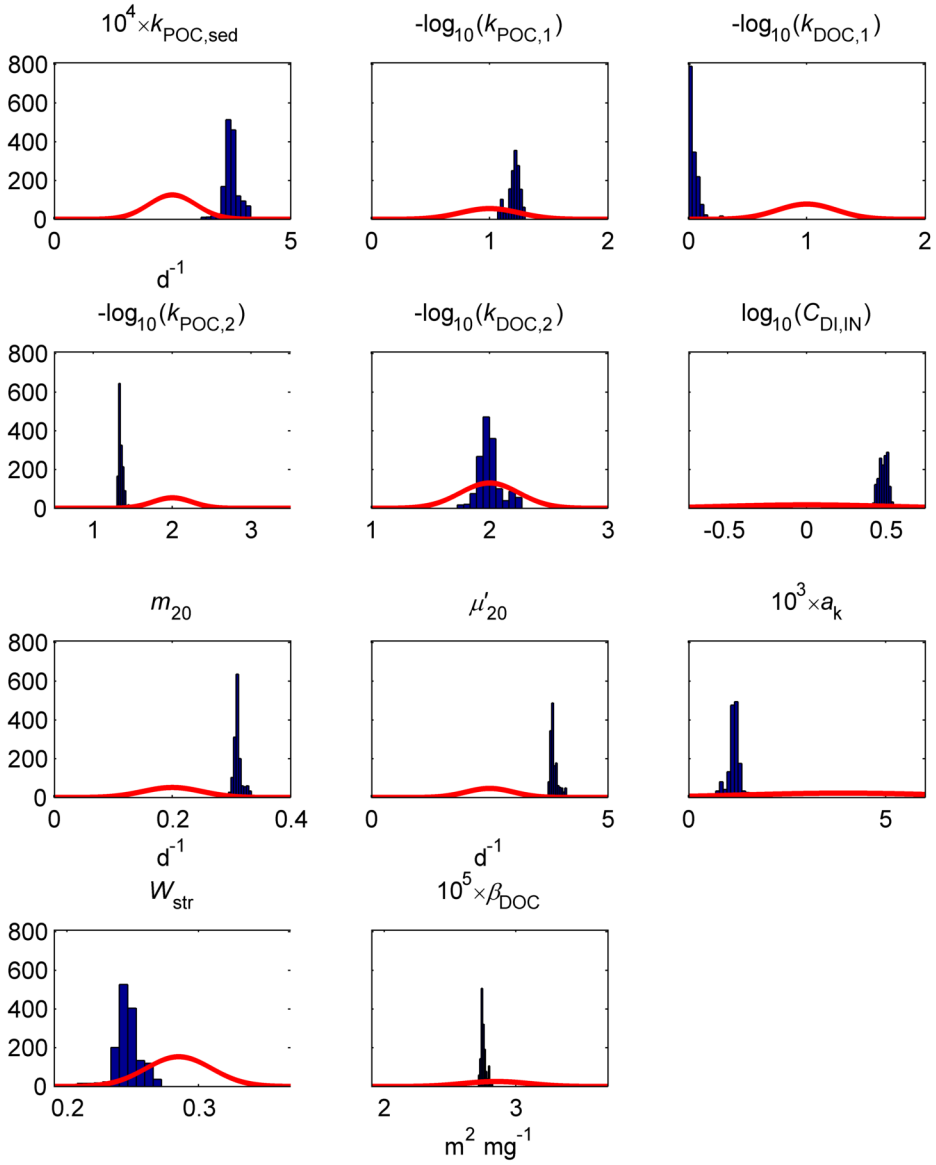

Figure S4. Histograms based on the posterior distributions of the 11 calibrated parameters (blue bars) estimated in the Markov chain Monte Carlo simulation with MyLake C using the gas exchange model by Tedford et al. (2014) and their prior probability distributions (red lines). The histograms were calculated using the latter half of the parameter chain with a length of 3000 iterations.

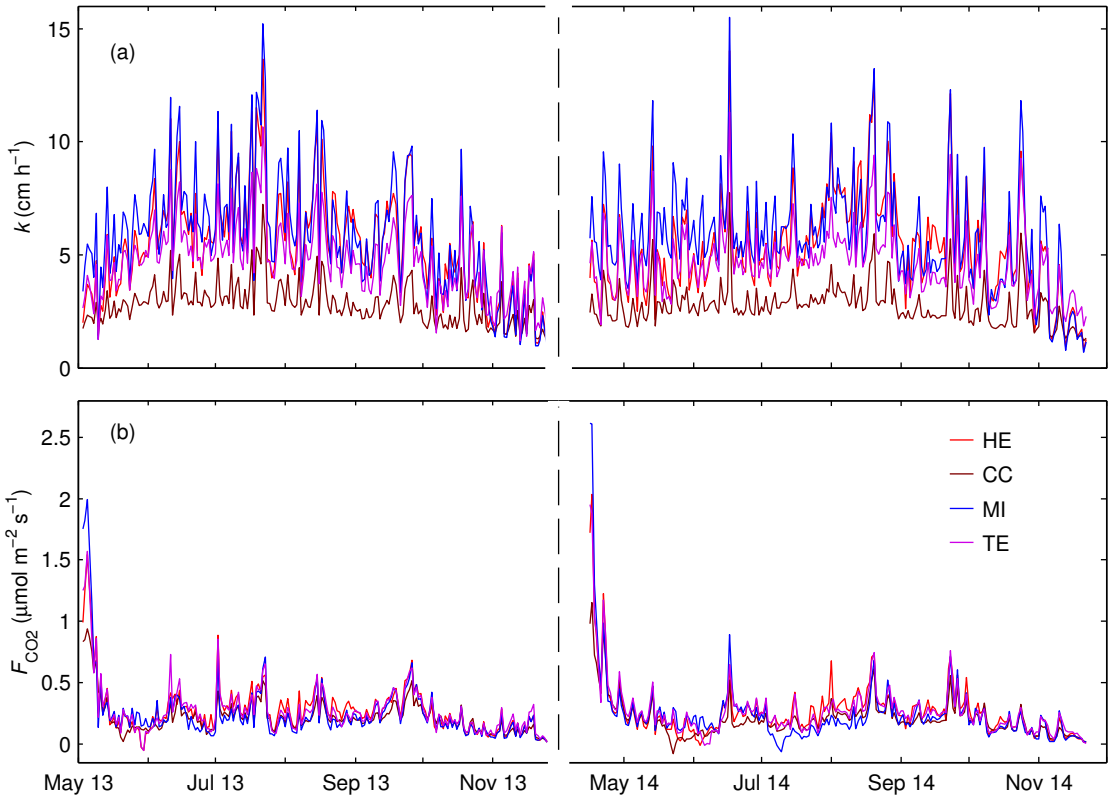

Figure S5. Simulated (a) gas transfer velocities for CO_2 ($cm\,h^{-1}$) and (b) air-water CO_2 fluxes ($\mu mol\,m^{-2}\,s^{-1}$) with each GEM in Lake Kuivajärvi during the open water seasons of 2013 and 2014.

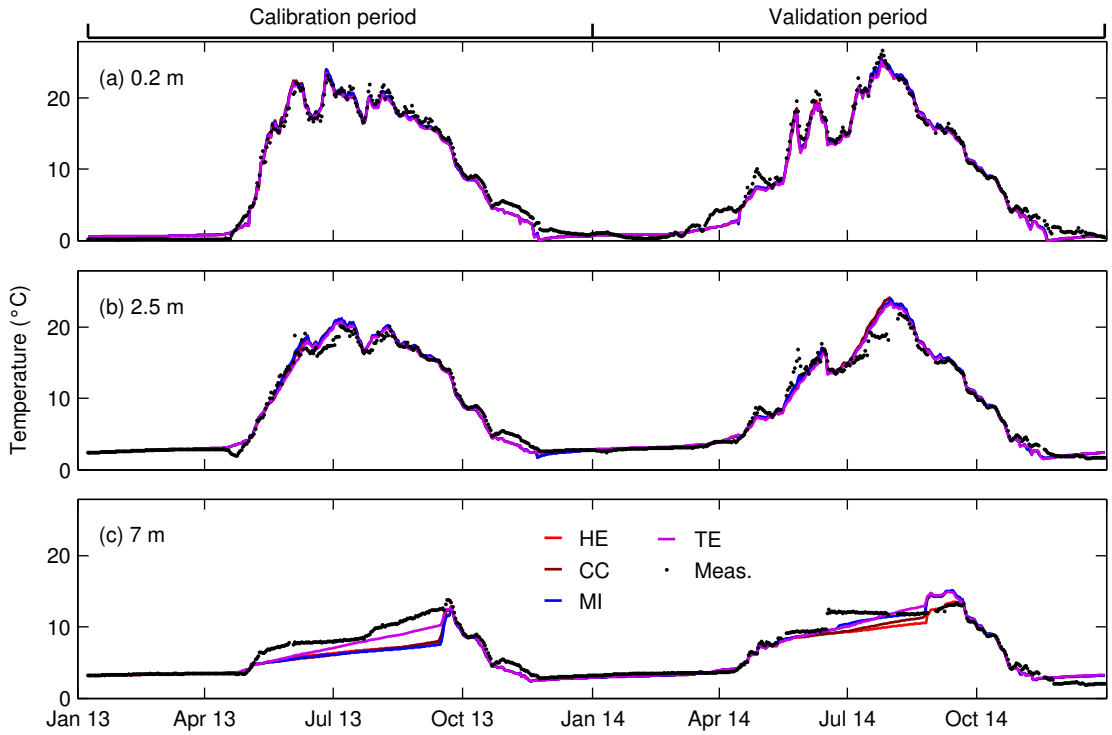

Figure S6. Simulation results for water temperature (°C) and the daily averages of automatic temperature measurements at depths of (a) 0.5 m, (b) 2.5 m, and (c) 7 m in Lake Kuivajärvi in 2013-2014.

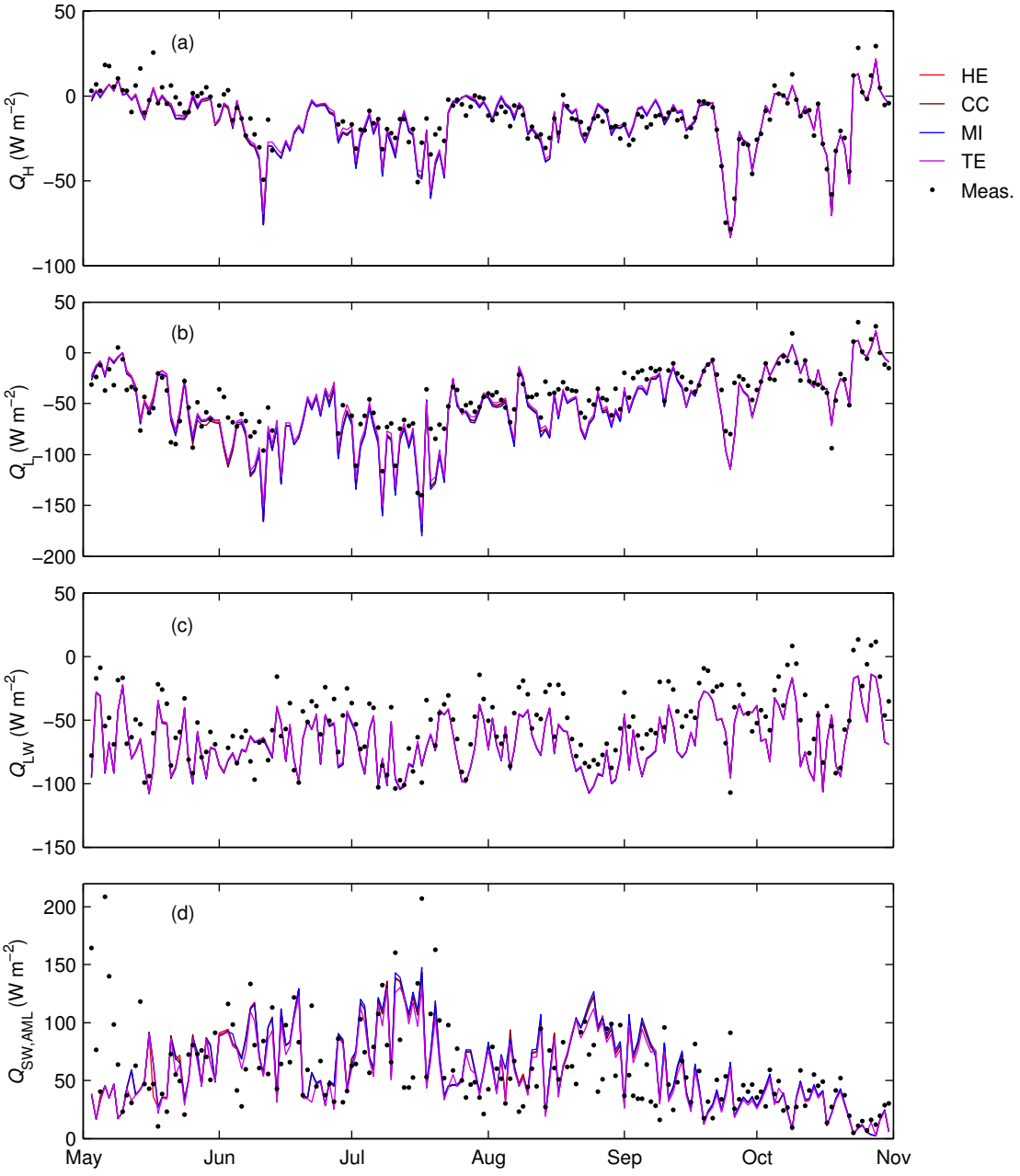

Figure S7. Simulated and measured daily (a) sensible heat fluxes ($\mathrm{W\,m^{-2}}$), (b) latent heat fluxes ($\mathrm{W\,m^{-2}}$), and (c) net longwave radiative heat fluxes ($\mathrm{W\,m^{-2}}$) at the surface of Lake Kuivajärvi and (d) simulated and calculated daily portions of shortwave radiative heat flux trapped in the active mixing layer of the lake ($\mathrm{W\,m^{-2}}$) in May–October 2013. The simulations were performed using each of the incorporated gas exchange models. Positive fluxes are directed into the water column.

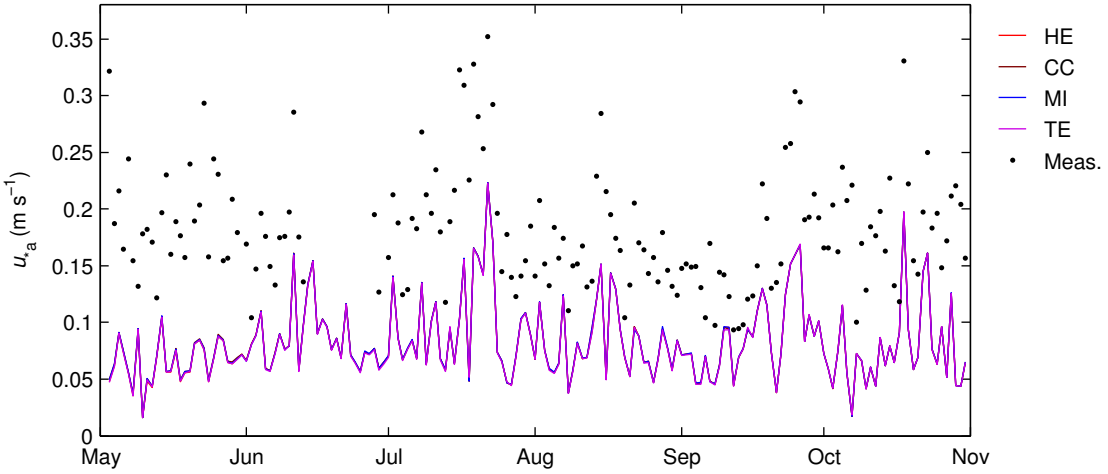

Figure S8. Daily atmospheric friction velocities ($\mathrm{m\,s^{-1}}$) simulated with each GEM and obtained from EC measurements over Lake Kuivajärvi. The differences in the simulated values of $u_{*\mathrm{a}}$ between GEMs, which were due only to different water surface temperatures, were very small.

Table S1. Statistical results[a] for the performance of the CO_2 simulations with the MyLake C application to Lake Kuivajärvi during the calibration and validation periods using different incorporated gas exchange models.

	R^2	p	RMSE[b]	NS	RMSD'*	B^*	n
Calibration (2013)							
Heiskanen							
0.5 m	0.70	< 0.001	23.03	0.63	−0.55	−0.26	246
2.5 m	0.74	< 0.001	24.08	0.62	0.57	−0.23	258
7 m	0.97	< 0.001	18.46	0.96	0.19	−0.06	276
Cole & Caraco							
0.5 m	0.69	< 0.001	21.22	0.68	−0.56	−0.054	246
2.5 m	0.79	< 0.001	18.31	0.78	−0.46	−0.088	258
7 m	0.97	< 0.001	19.50	0.96	0.19	−0.069	276
MacIntyre							
0.5 m	0.62	< 0.001	26.17	0.52	−0.62	−0.31	246
2.5 m	0.69	< 0.001	27.55	0.51	0.63	−0.30	258
7 m	0.97	< 0.001	18.49	0.96	0.18	−0.08	276
Tedford							
0.5 m	0.64	< 0.001	23.65	0.61	−0.60	−0.18	246
2.5 m	0.72	< 0.001	23.84	0.63	0.57	−0.20	258
7 m	0.97	< 0.001	19.47	0.96	0.19	−0.08	276
Validation (2014)							
Heiskanen							
0.5 m	0.41	< 0.001	17.41	−0.09	1.03	−0.14	191
2.5 m	0.77	< 0.001	20.20	0.67	0.55	−0.17	264
7 m	0.84	< 0.001	34.44	0.69	−0.40	−0.39	307
Cole & Caraco							
0.5 m	0.49	< 0.001	15.58	0.13	0.89	0.28	191
2.5 m	0.87	< 0.001	13.33	0.85	−0.36	−0.11	264
7 m	0.77	< 0.001	44.71	0.48	−0.49	−0.53	307
MacIntyre							
0.5 m	0.42	< 0.001	18.01	−0.16	1.05	−0.23	191
2.5 m	0.78	< 0.001	21.83	0.61	0.58	−0.24	264
7 m	0.76	< 0.001	43.74	0.50	−0.49	−0.50	307
Tedford							
0.5 m	0.40	< 0.001	17.11	−0.05	1.02	−0.03	191
2.5 m	0.59	< 0.001	25.99	0.45	0.74	0.02	264
7 m	0.68	< 0.001	42.75	0.52	−0.59	−0.36	307

[a]Coefficient of determination (R^2), root-mean-square error (RMSE), Nash–Sutcliffe efficiency (NS), normalized unbiased root-mean-square difference (RMSD'*), normalized bias (B^*).
[b]Units: CO_2, $\mathrm{mmol\,m^{-3}}$.

Table S2. Statistical results[a] for the performance of the simulation of surface heat fluxes (sensible heat flux (Q_H), latent heat flux (Q_L), and longwave radiative heat flux (Q_{LW})) and of the shortwave radiative heat flux trapped in the actively mixing layer ($Q_{SW,AML}$) in Lake Kuivajärvi over the periods 3 May–31 October 2013 using different gas exchange models incorporated in MyLake C. The simulated fluxes were evaluated against measured surface heat fluxes and against $Q_{SW,AML}$ based on the measured depths of the actively mixing layer.

	R^2	p	RMSE[b]	NS	RMSD'*	B^*	n
Q_H							
Heiskanen	0.84	< 0.001	7.34	0.80	0.42	−0.14	166
Cole & Caraco	0.83	< 0.001	7.50	0.79	0.43	−0.15	166
MacIntyre	0.83	< 0.001	7.54	0.79	0.43	−0.16	166
Tedford	0.85	< 0.001	6.87	0.82	0.41	−0.095	166
Q_L							
Heiskanen	0.82	< 0.001	18.65	0.57	0.58	−0.32	166
Cole & Caraco	0.83	< 0.001	18.37	0.58	0.56	−0.33	166
MacIntyre	0.83	< 0.001	18.75	0.56	0.56	−0.35	166
Tedford	0.83	< 0.001	16.49	0.66	0.52	−0.25	166
Q_{LW}							
Heiskanen	0.77	< 0.001	18.71	0.49	−0.48	−0.52	180
Cole & Caraco	0.77	< 0.001	18.79	0.49	−0.48	−0.53	180
MacIntyre	0.77	< 0.001	18.88	0.48	−0.48	−0.53	180
Tedford	0.77	< 0.001	18.43	0.51	−0.48	−0.51	180
$Q_{SW,AML}$							
Heiskanen	0.31	< 0.001	31.95	0.17	−0.91	0.024	180
Cole & Caraco	0.31	< 0.001	32.03	0.17	−0.91	0.021	180
MacIntyre	0.31	< 0.001	32.18	0.16	−0.91	0.050	180
Tedford	0.30	< 0.001	31.62	0.19	−0.90	−0.072	180

[a]Coefficient of determination (R^2), root-mean-square error (RMSE), Nash–Sutcliffe efficiency (NS), normalized unbiased root-mean-square difference (RMSD'*), normalized bias (B^*).
[b]Units: $\mathrm{W\,m^{-2}}$.

Table S3. Statistical results[a] for the performance of the simulation of water column CO_2 concentration at 0.2 m, gas transfer velocity for CO_2, and air-water CO_2 flux using different gas exchange models incorporated into MyLake C against the respective measured or calculated counterparts in Lake Kuivajärvi in 3 May–31 October 2013.

	R^2	RMSE	NS	RMSD'*	B^*	n
CO_2 concentration at 0.2 m[b]						
Heiskanen	0.63	21.70	0.35	−0.66	−0.47	161
Cole & Caraco	0.54	18.51	0.53	−0.69	−0.05	161
MacIntyre	0.45	26.49	0.027	−0.79	−0.59	161
Tedford	0.58	20.96	0.39	−0.69	−0.36	161
Gas transfer velocity for CO_2[b]						
Heiskanen	0.91	1.13	0.64	0.35	0.48	164
Cole & Caraco	0.99	0.19	0.95	0.11	0.19	164
MacIntyre	0.90	0.91	0.83	0.33	0.24	164
Tedford	0.45	3.65	−2.82	−0.76	−1.80	164
Air-water CO_2 flux[b]						
Heiskanen	0.46	0.23	0.38	−0.74	−0.26	158
Cole & Caraco	0.55	0.13	0.54	−0.67	0.082	158
MacIntyre	0.29	0.35	−0.035	−0.89	−0.49	158
Tedford	0.45	0.70	−0.026	−0.82	−0.60	158

[a]Coefficient of determination (R^2), root-mean-square error (RMSE), Nash–Sutcliffe efficiency (NS), normalized unbiased root-mean-square difference (RMSD'*), normalized bias (B^*).
[b]Units: CO_2 concentration, mmol m^{-3}; gas transfer velocity, cm h^{-1}; CO_2 flux, μmol m^{-2} s^{-1}.